Molecular Cell, Vol. 10, 857–869, October, 2002, Copyright ©2002 by Cell Press

Transcription Corepressor CtBP Is an NAD$^+$-Regulated Dehydrogenase

Vivek Kumar,[1,2,6] Justin E. Carlson,[4,6] Kenneth A. Ohgi,[2] Thomas A. Edwards,[4] David W. Rose,[3] Carlos R. Escalante,[4] Michael G. Rosenfeld,[2,5] and Aneel K. Aggarwal[4,5]

[1]Department of Biology Graduate Program
[2]Howard Hughes Medical Institute
School and Department of Medicine
[3]Department of Medicine
University of California, San Diego
La Jolla, California 92093
[4]Structural Biology Program
Department of Physiology and Biophysics
Mount Sinai School of Medicine
New York, New York 10029

Summary

Transcriptional repression is based on the selective actions of recruited corepressor complexes, including those with enzymatic activities. One well-characterized developmentally important corepressor is the C-terminal binding protein (CtBP). Although intriguingly related in sequence to D2 hydroxyacid dehydrogenases, the mechanism by which CtBP functions remains unclear. We report here biochemical and crystallographic studies which reveal that CtBP is a functional dehydrogenase. In addition, both a cofactor-dependent conformational change, with NAD$^+$ and NADH being equivalently effective, and the active site residues are linked to the binding of the PXDLS consensus recognition motif on repressors, such as E1A and RIP140. Together, our data suggest that CtBP is an NAD$^+$-regulated component of critical complexes for specific repression events in cells.

Introduction

Transcriptional repression is mediated by a wide variety of DNA binding transcription factors, serving critical roles in development and homeostasis. In turn, these repressors often appear to require association with corepressors to mediate inhibition of gene transcription (Gray and Levine, 1996; Pazin and Kadonaga, 1997; Tyler and Kadonaga, 1999). These corepressors include closely related factors present in multiple complexes, such as histone deacetylases (HDACs), that link repression to chromatin structure and protein modification. Many enzymatic activities are linked to recruited cofactor complexes: these include acetylation and phosphorylation, ADP ribosylation, and methylation (Cheung et al., 2000; Jenuwein and Allis, 2001).

The discovery of the C-terminal binding protein (CtBP), because of its sequence homology to D2-hydroxyacid dehydrogenases, potentially presents another molecular enzymatic strategy for repression. CtBP was initially identified as a partner of adenovirus E1A protein and derives its name from its ability to bind a PXDLS sequence at the E1A C terminus (Boyd et al., 1993; Schaeper et al., 1995). The binding of CtBP to E1A results in the loss of CR1-mediated transactivation, behavior identical to that of a transcriptional repressor. Genetic support for the ability of CtBP to function in vivo as a transcription corepressor was provided by experiments carried out in *Drosophila*. *Drosophila* CtBP (dCtBP) is maternally expressed and uniformly distributed throughout the early embryo. Mutations in dCtBP cause severe segmentation and patterning defects that have been attributed to the combined loss of repression activities of *Knirps*, *Krüppel*, and *Snail*; factors critical for early development and repression of genes such as *even skipped*, *rhomboid*, and *fushi tarazu* (Nibu et al., 1998a, 1998b; Poortinga et al., 1998). All three of these sequence-specific repressors contain PXDLS-related motifs that have been shown in vitro and in vivo to be important in recruiting dCtBP. CtBP1 and CtBP2, a second highly related factor in vertebrates, have been linked to a host of disparate transcription factors including several that are important in cellular proliferation, homeostasis, and development by a conserved PXDLS-like motif (Chinnadurai, 2002).

In contrast to other corepressors, such as N-CoR/SMRT and mSin3, which have no intrinsic enzymatic activity but instead recruit enzymatic components such as HDACs (Glass and Rosenfeld, 2000), CtBP is set apart by its unexpected sequence similarity to D2-hydroxyacid dehydrogenases (D2-HDHs) (Schaeper et al., 1995; Turner and Crossley, 2001). Remarkably, most of human CtBP1 sequence (except for ~90 residues at the C terminus) can be aligned with this subfamily of NAD$^+$-dependent dehydrogenases, which includes D-glycerate dehydrogenase (D-GDH) and D-lactate dehydrogenase (D-LDH) among others (Goldberg et al., 1994; Stoll et al., 1996). This unusual similarity to D2-HDHs has prompted speculation that CtBP may also bind NAD$^+$ and possess dehydrogenase activity—relevant to its corepression function. However, initial attempts to define NAD$^+$ binding and dehydrogenase activity in CtBP have been unsuccessful (Schaeper et al., 1995). The lack of a known D2-hydroxyacid substrate, and recent reports that CtBP can induce fission of Golgi membrane by acetylating lysophosphatidic acid (Spanfò et al., 1999; Weigert et al., 1999), and that RIBEYE, a component of ribbon synapses, is a splice variant of CtBP2 (Schmitz et al., 2000), have led to further uncertainty regarding the actions of CtBP.

In this manuscript, we show that CtBP is a bone fide D2-hydroxyacid dehydrogenase, with a characteristic dumbbell shape and a deep, narrow cleft for both NAD$^+$ and substrate binding. We further demonstrate that the dehydrogenase domain is necessary and sufficient to mediate repression and identify the NAD$^+$ and putative substrate interactions based on the structure of the dehydrogenase domain determined in the presence of NAD$^+$. Furthermore, we show that E1A binding to CtBP

[5]Correspondence: aggarwal@inka.mssm.edu (A.K.A), mrosenfeld@ucsd.edu (M.G.R.)
[6]These authors contributed equally to this work.

is NAD^+ dependent, requiring active site residues and a functional dimer. The catalytic residues are also required for RIP140-dependent repression of retinoic acid receptor (RAR). Together, these initial structural and biochemical results suggest an allosteric mechanism for recruitment of CtBP to its consensus recognition motif for specific repression events in cells.

Results

CtBP Is a Functional Dehydrogenase

We first asked whether CtBP is a functional dehydrogenase. Dehydrogenase activity can be assayed by quantitating change of NADH to NAD^+ or vise versa, which can be monitored by loss or gain of absorbance at 340 nm (Adams et al., 1973). Most dehydrogenases have a strict substrate specificity; however, they will catalyze nonoptimal substrates at slower rates. We used an assay that coupled the reduction of pyruvate to lactic acid with the oxidation of NADH to NAD^+. For these experiments we purified CtBP from baculovirus-infected SF9 cells, yielding essentially a homogenous protein (Figure 1C). CtBP was able to catalyze this reaction in a dose-dependent manner (Figure 1A). Even though the reaction was inefficient, it is specific to CtBP, as both an equivalent volume of uninfected SF9 cell extract (Figure 1B), and a catalytic site mutant of CtBP (Figure 6D) were not able to catalyze the reaction. In addition, the reactions required the presence of pyruvate, demonstrating that the substrate is not CtBP itself, anything in the SF9 extract, or buffer (Figure 1B). Thus using a nonoptimal substrate, we were able to demonstrate that CtBP is a functional dehydrogenase.

The Dehydrogenase Domain Alone Is a Repressor

All but the last 90 aa of 440 residue hCtBP1 has significant homology to D2-HDHs. Having shown that CtBP is a functional dehydrogenase, we sought to determine what role the dehydrogenase domain alone has in repression and recruitment of CtBP to a PXDLS motif. We used two independent assays to test whether the CtBP dehydrogenase domain is a repressor. When tethered to DNA by a Gal4 DNA binding domain (DBD), the dehydrogenase domain of CtBP represses as well as full-length CtBP (Figure 1D, compare lanes 2 and 3), and the last 90 aa of CtBP1 (C′) has no significant repressive activity in this assay (Figure 1D, lane 4). In another assay, we used CtBP to repress Gal4DBD/E1A-mediated activation from a UAS/tk luciferase. We also used the C′ (last 78 aa) of E1A, which was used to clone CtBP in a two-hybrid screen and is not a repressor until CtBP is overexpressed. The dehydrogenase domain only was able to repress Gal4/E1A C′-mediated transcription as well as full-length CtBP1 or CtBP2 (Figure 1E, compare lane 4 with lanes 2 and 3).

Because the dehydrogenase domain alone is capable of repressing Gal4/E1A, we tested whether it could interact with E1A. We used GST E1A C′ (the same region used in experiments in Figure 1E) and in vitro transcribed and translated (TnT) CtBP full-length or dehydrogenase domain to test direct binding. The dehydrogenase domain alone is sufficient to interact with E1A (Figure 1F) as robustly as full-length CtBP1 or CtBP2. Furthermore, this interaction is specific to the PXDLS motif of E1A, as a peptide containing this motif is able to effectively compete with this interaction. Thus, the dehydrogenase domain of CtBP is sufficient to interact with PXDLS motif and mediate functional repression.

Structure of CtBP

Given that the dehydrogenase domain of CtBP is a functional dehydrogenase and that it alone mediates repression, we set out to determine its structure. We expressed and purified the 28–353 residue minimal domain from bacteria in the presence of NAD^+, and crystals of the complex were obtained from solutions containing sodium formate and magnesium acetate. The structure was solved by multiwavelength anomalous diffraction (MAD) method (Hendrickson, 1991) using selenomethionine-labeled protein expressed in a strain of *E.coli* that is methionine auxotrophic (Table 1). The current model, refined to 1.95 Å resolution, includes residues 28–352 with good stereochemistry. The crystallographic asymmetric unit contains a CtBP monomer that forms extensive dimer contacts with a crystallographic 2-fold related copy.

CtBP is thus a dimer, where each monomer is divided into large and small domains separated by a flexible hinge region (Figure 2). A cleft at the confluence of the two domains provides binding sites for NAD^+ as well as a putative substrate. Because all of the NAD^+ binding residues stem from the large domain, it has been called the NAD^+ or coenzyme binding domain in previous D2-HDH structures. The small domain will be referred to as the substrate binding domain, which is globular in shape ($\sim 32 \times 25 \times 29$ Å) and composed of residues from both the N (aa 27–121) and C terminus (aa 327–352). The NAD^+ binding domain is contiguous in polypeptide (aa 125–318), elongated in shape ($\sim 53 \times 33 \times 39$ Å), and mediates most of the dimerization contacts (Figure 2). The dimerization interface is extensive, burying ~ 3368 Å^2 of solvent accessible surface area per monomer (Figure 2B). The hinge between the NAD^+ and substrate binding domains is composed of two segments, amino acids 122–124 and 319–326.

The NAD^+ binding domain is the most similar to that of other D2-HDHs (Dengler et al., 1997; Goldberg et al., 1994; Lamzin et al., 1994; Schuller et al., 1995; Stoll et al., 1996), composed of a parallel β sheet (βA-βG) flanked on both sides by α helices (αA-αH). The connectivity resembles a Rossmann or a dinucleotide binding fold that occurs widely in NAD^+-dependent dehydrogenases (Rao and Rossmann, 1973). This similarity in connectivity reflects the maintenance of residues mediating NAD^+ binding as well as the conservation of a GXGXXG(17X)D signature motif. In comparing CtBP against other D2-HDH structures, the most pronounced deviation is the omission of a 15 residue insert found between amino acids 265 and 281 in D-LDH and amino acids 263 and 279 in D-2-hydroxyisocaproate dehydrogenase (D2-HicDH) (see for instance, Dengler et al., 1997; Stoll et al., 1996). The exclusion of this segment in CtBP may be important in allowing the binding of the PXDLS sequence (discussed below). Otherwise, the CtBP NAD^+ binding domain superimposes extremely well with other D2-HDHs, with rmsds ranging from 1.1 to 1.2 Å. The

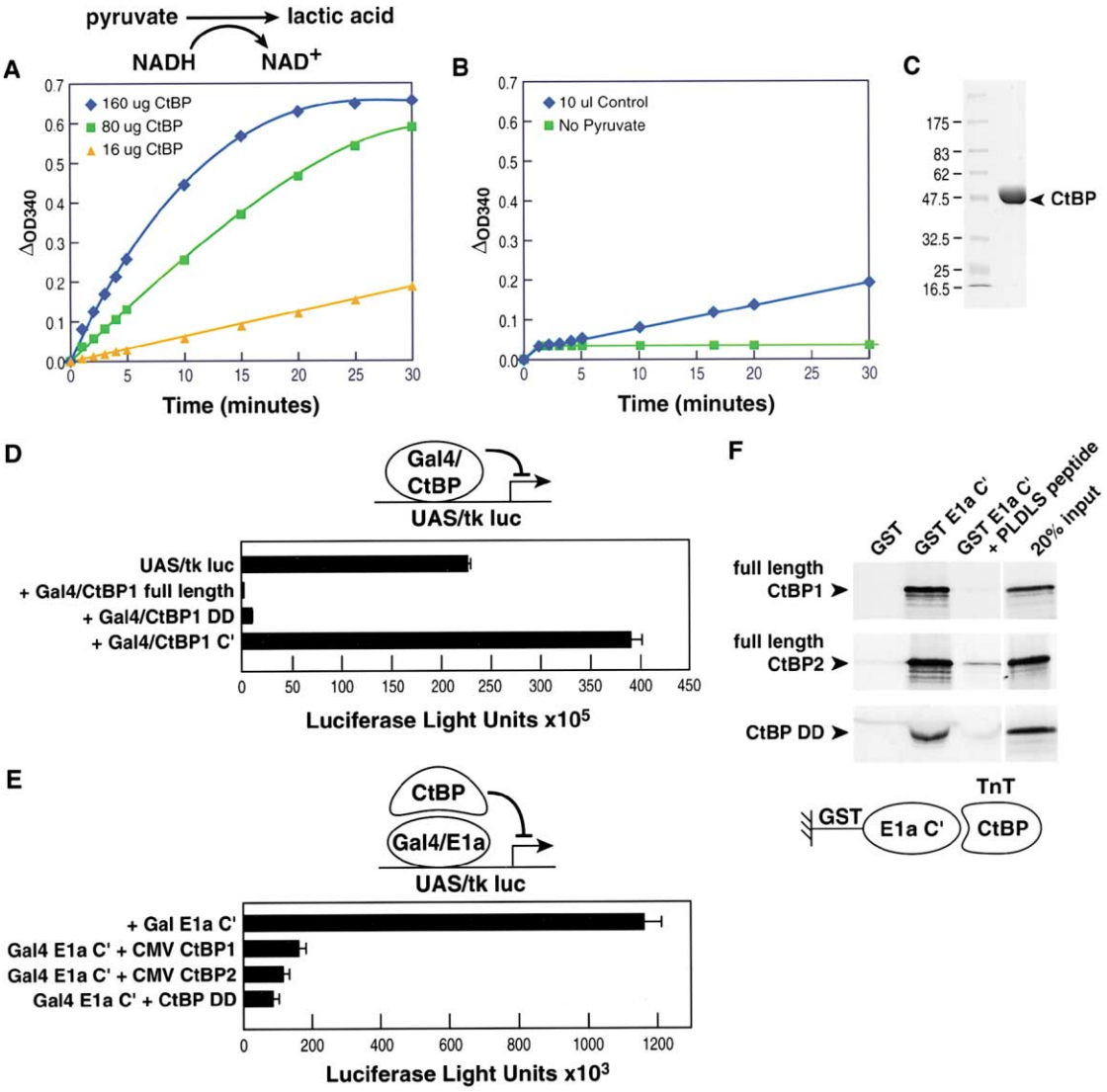

Figure 1. CtBP Is a Functional Dehydrogenase

(A) Dehydrogenase assays were performed to measure the conversion of pyruvate to lactic acid and coupled oxidation of NADH to NAD^+ as described in Experimental Procedures. Varying amounts of full-length CtBP purified from baculovirus-infected SF9 cells were incubated with 20 mM pyruvate and the change in absorbance at 340 nm was measured over time.

(B) As control an equivalent volume of SF9 extract from uninfected cells was used as well as a reaction without any substrate.

(C) Coomassie stain of the CtBP is shown.

(D–F) The dehydrogenase domain of CtBP is sufficient to bind PXDLS motif and mediate repression. (D) When fused to the Gal4/DBD full-length CtBP and dehydrogenase domain (DD) alone can repress transcription (lane 2 and 3, respectively) from a UAS/tk luciferase reporter. The C terminus of CtBP1 is not capable of being a repressor as a gal fusion (lane3). (E) The dehydrogenase domain can also repress transcription when recruited by gal4/E1A C′. The dehydrogenase domain can effectively repress transcription as well as full-length CtBP or CtBP2 (compare lane 3 with 1 and 2). (F) The dehydrogenase domain binds to GST/E1A C′ equivalently as full-length CtBP1 and CtBP2. This interaction can be disrupted by the addition of a peptide containing the PXDLS motif (lane 3). Results are shown as mean ± standard deviation and are representative of three independent experiments.

substrate binding domain is more variable with rmsds ranging from 1.3 to 1.65 Å. This variability is further enhanced by loops extending into the active site cleft, consistent with different substrate specificities.

Active Site Cleft

NAD^+ binds in the active site cleft in the characteristic bent L-shaped configuration seen in other NAD^+-dependent dehydrogenases (Eklund and Branden, 1987). The adenine moiety is oriented toward the entrance to the cleft while the nicotinamide ring is more deeply buried toward the substrate binding pocket (Figure 2A). Residues Glu204, Arg184, and Asp290 play key roles in fixing the adenine ribose, the pyrophosphate group, and the carboxyamide group of the nicotinamide, respectively (Figure 3A). In addition to side chain atoms, main chain carbonyl (Cys237 and Thr264) and amide (Arg184, Val185, and Trp318) groups also contribute to NAD^+ binding (Fig-

Table 1. Data Collection, Phasing, and Refinement Statistics

Data Collection				
	Se-Edge	Se-Peak	Se-Remote	Native
Wavelength (Å)	0.97957	0.97941	0.966859	1.14072
Resolution (Å)	2.8	2.8	2.8	1.95
Number of reflections				
Measured	133,207	133,033	132,781	173,537
Unique	9,549	9,534	9,531	52,854
Data coverage (%)	99.2 (100)	99.0 (99.8)	99.0 (100)	99.0 (94.1)
R_{merge} (%)[a,b]	6.1 (30.8)	8.0 (32.1)	6.3 (34.6)	4.1 (31.4)
I/σ	37.4 (9.6)	26.5 (9.4)	37.6 (11.6)	23.8 (2.0)
MAD Phasing Statistics				
Number of sites	5	5	5	–
FoM (centric/acentric) 3.2 Å[c]	0.9484/0.5924			
FoM (DM) 2.25 Å[d]	0.9612			
Phasing power	2.2	2.6	2.7	–
Refinement Statistics				
Resolution range (Å)				50–1.95
Reflections, $F > 2\sigma$ (F)				50,259
R_{cryst} (%)[e]				21.1
R_{free} (%)[f]				25.3
Non-hydrogen atoms				
Protein				2516
NAD^+				44
Acetate				4
Water				414
Rmsd				
Bonds (Å)				0.008
Angles (°)				1.53
Average B factor (Å^2)				36.9

[a] Values for outermost shell are given in parentheses.
[b] $R_{merge} = \Sigma |I - \langle I \rangle| / \Sigma I$, where I is the integrated intensity of a given reflection.
[c] FoM = mean figure of merit computed to 3.2 Å.
[d] FoM = overall mean figure of merit at 2.25 Å after density modification.
[e] $R_{cryst} = \Sigma ||F_o| - |F_c|| / \Sigma |F_o|$.
[f] R_{free} was calculated using 10% of data excluded from refinement.

ure 3A). The structure reveals why glycines at positions 181 and 183 (*GXGXXG*(17X)D) are critical for NAD^+ binding, since substitution by any other amino acids at these positions would cause steric clashes with the bridging pyrophosphate bridge. The adenine is nestled in a hydrophobic cavity defined by residues Pro205 and Tyr206, with its N7 atom accepting a hydrogen bond from Asn240 (Figure 3A).

A His/Glu(Asp)/Arg triad is conserved in all D2-HDHs and implicated as the center for substrate binding and dehydrogenase activity. The structurally equivalent residues in CtBP are His315, Glu295, and Arg266. The histidine is postulated to be the acid/base catalyst, with the glutamate/aspartate helping to lower the pKa of the histidine to stabilize it in a protonated state. The arginine is proposed to polarize the 2-hydroxyl of the substrate for catalysis. While a biologically relevant substrate for CtBP remains to be identified, the structure provides valuable insights into the nature of a putative substrate. In particular, a superposition with D2-HicDH/NAD^+/substrate ternary complex results in positioning 2-oxoisocaproate in the CtBP active site (Figure 3B) (Dengler et al., 1997). The nonaliphatic portion of 2-oxoisocaproate is found to be accommodated remarkably well in the CtBP active site, and a plausible hydrogen bonding scheme can be derived in which Arg97 and Ser100 form hydrogen bonds with the terminal carboxylate group, and Arg266 is in a position to form a bond with the 2-hydroxyl. Interestingly, Arg97 and Ser100 are primarily hydrophobic residues in other D2-HDHs. In D2-HicDH, the terminal carboxylate is instead recognized by Tyr100, which is an alanine (Ala123) in CtBP (Figure 3B). Thus, CtBP may use a different set of amino acids to fix the orientation of a D-2-hydroxyacid substrate in its active site as compared to other D2-HDHs. His315 and Arg266 are <4 Å from the 2-hydroxyl group of the modeled substrate. The aliphatic portion of modeled 2-oxoisocaproate clashes with Trp318 that emanates from the CtBP NAD^+ binding domain and His77 that extends from the substrate binding domain. Both of these residues are unique to CtBP and probably contribute to its substrate specificity (Figure 3B). The steric clashes with these residues suggest that CtBP probably binds a 2-hydroxyacid substrate that is somewhat smaller in the "R" group than D-2-hydroxyisocaproate. Also, the lack of basic residues around this region corresponding, for instance, to Arg60 in phosphoglycerate dehydrogenase (PGDH) (Schuller et al., 1995) suggests that CtBP probably binds to a substrate lacking a phosphate group.

Curiously, we observe an acetate ion in the CtBP sub-

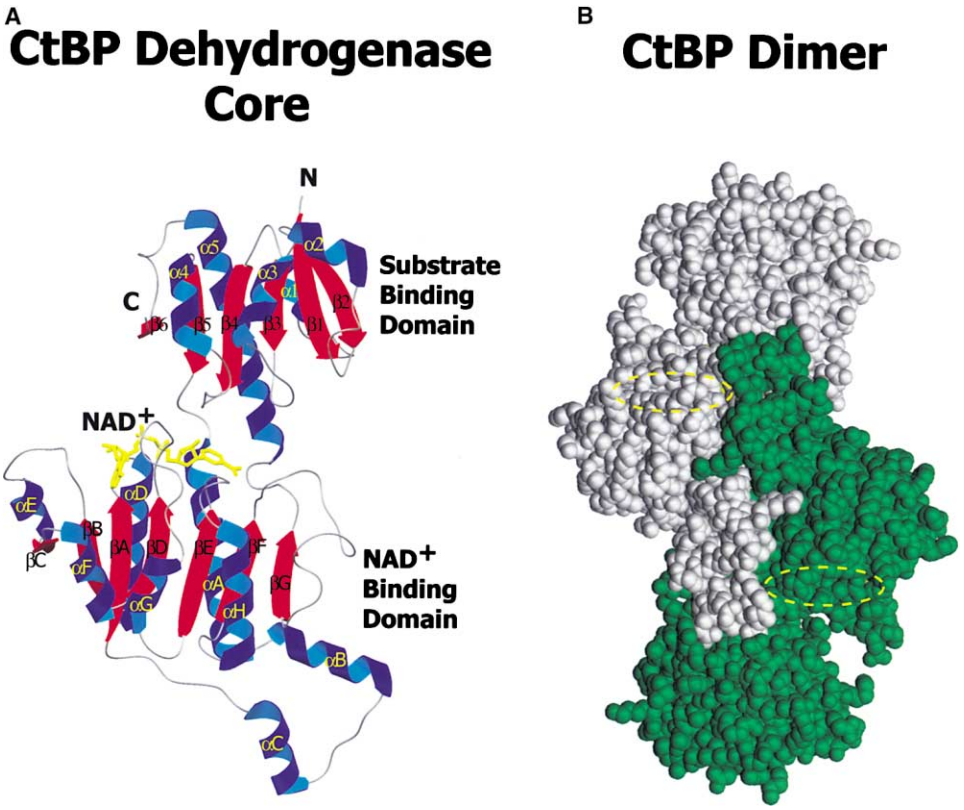

Figure 2. CtBP Structure

(A) The dehydrogenase domain contains a substrate binding domain linked via a flexible hinge to the NAD+ binding domain. NAD+ (yellow) binds in the active site cleft in a bent L-shaped configuration.

(B) The van der Waals (vdw) surface of a CtBP dimer. One monomer is drawn in gray and the other in green. The gray monomer is related to the monomer in (A) by rotation of ~81°, roughly along the vertical axis of the paper, to give a view of the CtBP dimer down the 2-fold axis. The NAD+ molecules are hidden from view by the vdw surface; their approximate positions are indicated by dashed ovals. Note, the NAD+ binding domain makes the majority of dimeric interactions.

strate binding pocket (Figure 3B), hydrogen bonded to His315 (2.8 Å), Arg266 (2.8 and 2.9 Å), and Arg97 (2.8 Å). This prompted us to test whether CtBP could catalytically modify an acetyllysine residue on a histone H3-derived peptide, but we found no evidence. An acetate ion is similar to a 2-hydroxyacid substrate in containing a terminal carboxylate group, but it lacks the 2-hydroxyl group. The acetate ion, present in the crystallization mix and critical for CtBP crystallization, is bound in an orientation different from what we expect for a real substrate: its second carboxylate oxygen occupies the position anticipated for oxidation/reduction of the 2-hydroxyl (Figure 3B). The acetate's small size and structural similarity to 2-hydroxyacids appear to permit tight binding in the CtBP active site.

E1A Is Recruited through a NAD+-Dependent Conformational Change

Conformational change on NAD+ binding is a key feature of NAD+-dependent dehydrogenases (Eklund and Branden, 1987). In the majority of cases, NAD+ binding causes a narrowing of the active site cleft due to a movement of the substrate binding domain toward the cleft. The structures of holo- and apo-FDH, for instance, differ in the location of the substrate binding domain, corresponding to a 7.5° rotation around the hinge region (Lamzin et al., 1994). Similar rigid body motion has been described for other NAD+-dependent dehydrogenases, where the apo form has been termed the "open" conformation and the NAD+-bound form as the "closed" conformation (Grau et al., 1981; Lamzin et al., 1994). In comparing our structure against other NAD+-bound D2-HDHs, the active site cleft is particularly narrow. For example, the average distance across the cleft (measured between residues 101 and 266, and 78 and 294) is ~10 Å, as compared to ~16 Å in D-LDH and ~13 Å in D-HicDH. Only FDH has a narrower active site cleft (~8 Å), which may reflect the small size of its formate ion substrate (Lamzin et al., 1994).

A comparison with apo-D-GDH structure—based on the alignment of NAD+ binding domains—suggests that the CtBP substrate binding domain moves toward the closed conformation by a rotation of ~5° (Figure 4A). To evaluate the potential role of NAD+-induced conformational change in protein-protein interactions, we evaluated the effects of adding NAD+ to binding of E1A to CtBP. We found that in the presence of NAD+, CtBP bound to E1A much more efficiently (Figure 5A). This NAD+ dependency was observed both with the full-length CtBP, as well as with the isolated dehydrogenase domain (Figure 5A). These data strongly imply that NAD+

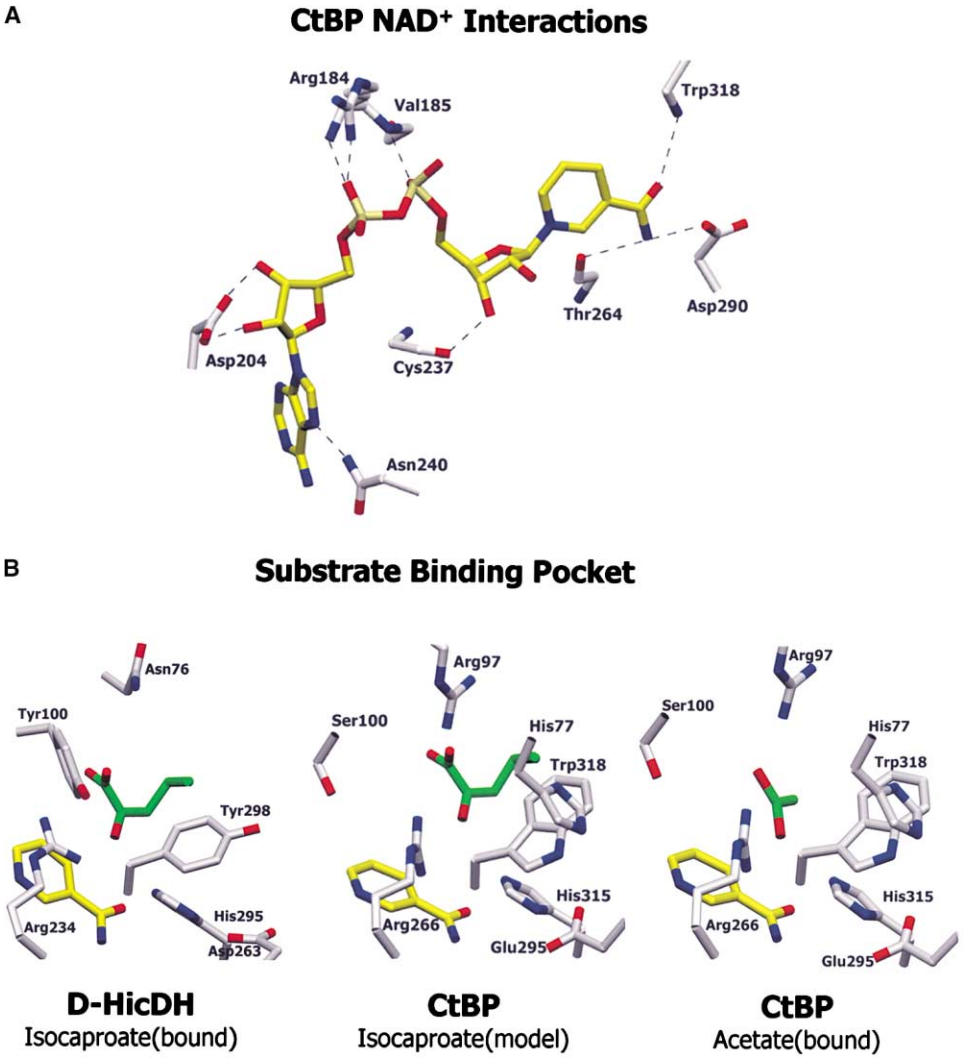

Figure 3. CtBP Interactions

(A) Interactions between bound NAD^+ (yellow) and CtBP residues. Both side chain (Arg184, Asp204, Asn240, and Asp290) and main chain (Arg184, Val185, Cys237, Thr264, and Trp318) atoms make hydrogen bonds (dotted lines) with NAD^+.

(B) The 2-oxoisocaproate substrate (green) bound to D-HicDH (left panel) is positioned in CtBP (middle panel) based on superposition of the two enzymes. The His315(295)/Glu295(Asp263)/Arg266(234) catalytic triad is conserved between the enzymes, but the other residues lining the substrate binding pocket are different. The nicotinamide ring of NAD^+ is included in the panels to aid orientation with respect to (A). The CtBP structure reveals a bound acetate ion (right panel). The carboxylate group of the acetate ion is oriented differently from the carboxylate of the modeled 2-oxoisocaproate molecule (middle panel).

binding to CtBP causes a conformational change necessary for binding of the PXDLS motif.

Recently it has been reported that the ratio of NAD^+ and NADH can regulate the function of DNA binding transcription factors (Rutter et al., 2001). In addition, Zhang et al. (2002) have reported that CtBP binds E1A two to three orders of magnitude better in the presence of NADH than NAD^+. Given these intriguing findings, we tested whether E1A binding to CtBP is regulated differently by NADH versus NAD^+. We quantitated the interaction between TnT CtBP and GST-E1A under different concentrations of NAD^+, NADH, and various NAD^+-like molecules. Both NAD^+ and NADH were found to be equally effective in stimulating E1A-CtBP interaction, with concentrations required for half-maximal stimulation in the 1–10 μM range (Figures 5E and 5F). ADP-ribose, an NAD^+/NADH analog lacking the nicotinamide ring, also increased E1A-CtBP interaction, though the concentration required for half-maximal stimulation was ~10× higher than that for NAD^+ or NADH (Figure 5E). Titration with β-nicotinamide mononucleotide (NMN) or the nicotinamide ring alone, however, was not sufficient to stimulate E1A-CtBP interaction. Thus, in our assay, NAD^+ and NADH appear to be equally effective in triggering the conformational switch in CtBP for E1A binding. Furthermore, compounds such as ADP-ribose that are capable of causing conformational change, from open to closed state, in dehydrogenases can also mediate E1A binding.

To appraise this NAD^+/NADH-dependent conforma-

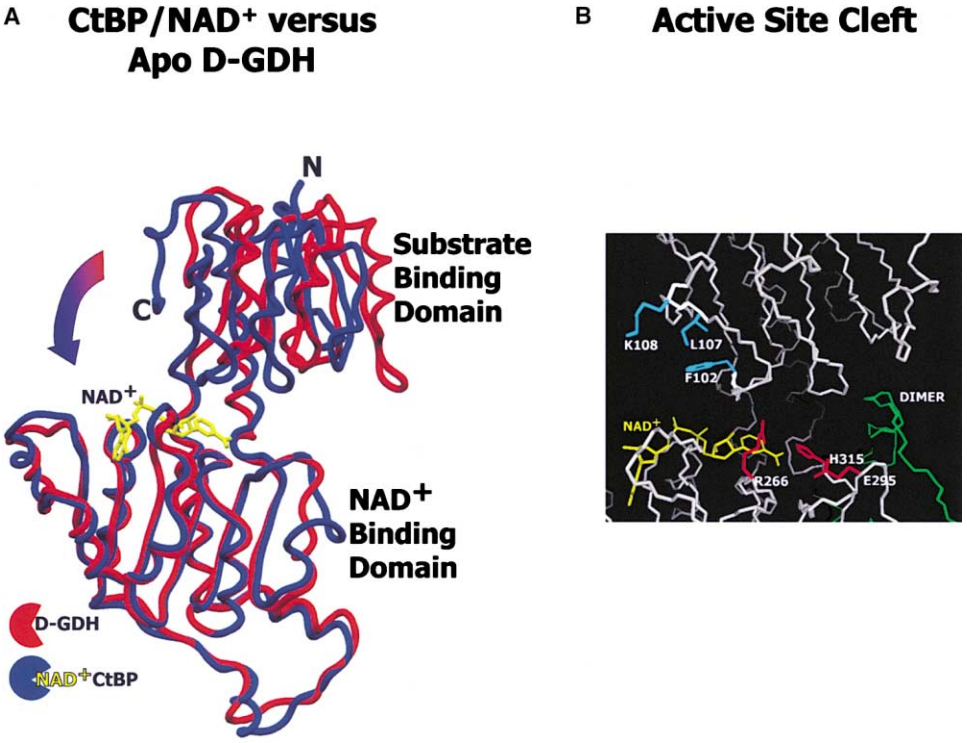

Figure 4. Conformational Change and PXDLS Binding

(A) The CtBP/NAD+ complex (blue) is compared to apo-D-GDH (red) solved in the absence of NAD+ (Goldberg et al., 1994). The superposition, based on NAD+ binding domains, reveals a relative displacement in the substrate binding domains, marking "open" and "closed" states. The N and C termini of CtBP are labeled. NAD+ bound to CtBP is drawn in yellow.

(B) Location of residues mutated in $Cleft_{mut}$ (blue) and Cat_{mut} (red). $Cleft_{mut}$ mutations of residues F102, I107, and K108, lining a cavity at one the active site cleft, do not affect E1A binding or repression function. Cat_{mut} mutations of the catalytic triad residues (H315, E295, and R266) and D290 disrupt both E1A binding and repression activity. The PXDLS recognition motif is hypothesized to bind close to these catalytic residues, aided by interactions from a loop (green) from the 2-fold related subunit. The bound NAD+ is drawn in yellow.

tional change further, we undertook limited proteolysis of TnT CtBP in the absence and presence of varying concentrations of NAD+ and NADH. The digestion was carried out with the nonspecific protease papain that has been used widely to probe the configuration of modular proteins. CtBP in the presence of NAD(H) is resistant to papain digestion, producing a very stable ~40 kDa fragment, which we used as qualitative assay for NAD(H)-dependent conformational change (Figure 5G). Using this assay, we determined the concentration of NAD+ and NADH at which the resistant 40 kDa fragment was produced. Consistent with our E1A binding data, the protease digestion showed a conformational switch between 1 and 10 μM NAD+ and NADH, with both compounds behaving identically (Figure 5G). Thus using two independent assays, we could not detect any difference in NAD+- and NADH-induced conformational change of CtBP translated in an in vitro mammalian system.

The PXDLS Motif Interacts Directly with the Active Site Residues

In order to further test our hypothesis that the PXDLS motif makes direct contacts with the CtBP dehydrogenase domain, we introduced point mutations, based on the crystal structure, to disrupt NAD+ binding (NAD_{mut}), as well as the substrate/catalytic pocket (Cat_{mut}), the dimerization function (Dim_{mut}), and a cavity at one end of active site cleft ($Cleft_{mut}$). The mutations included D204A, G181V, and G183V for NAD_{mut}, and H315A, E295A, R266A, and D290A for Cat_{mut}. Because of the extensive dimer interface two sets of mutations were generated: R141A, R142A, R163A, and R171A to disrupt critical salt links and hydrogen bonding across the interface ($Dim1_{mut}$), and C134Y, N138R, R141E, and L150W to introduce steric and electrostatic repulsion across the interface ($Dim2_{mut}$). $Cleft_{mut}$ included K108A, F102A, and I107A mutations to disrupt residues lining a cavity near the entrance to the active site cleft that we initially speculated might interact with the PXDLS motif (Figures 2B and 4B). As expected, NAD_{mut} strongly inhibited CtBP's ability to bind E1A (Figure 5A), consistent with the NAD+/NADH dependency observed above with the native enzyme. Unexpectedly, however, Cat_{mut} and Dim_{mut} also severely compromised the ability of CtBP to bind E1A, while $Cleft_{mut}$ did not affect interaction with E1A (Figure 5A). Similar results were obtained with CtBP holoprotein and the isolated dehydrogenase domain. To test whether the PXDLS motif actually competes with substrate binding, we measured CtBP's dehydrogenase activity in the presence of a PXDLS peptide and observed little effect. Taken together, the mutagenesis data suggest that the PXDLS motif is accommodated outside of the substrate binding pocket but sufficiently close to it to interact with

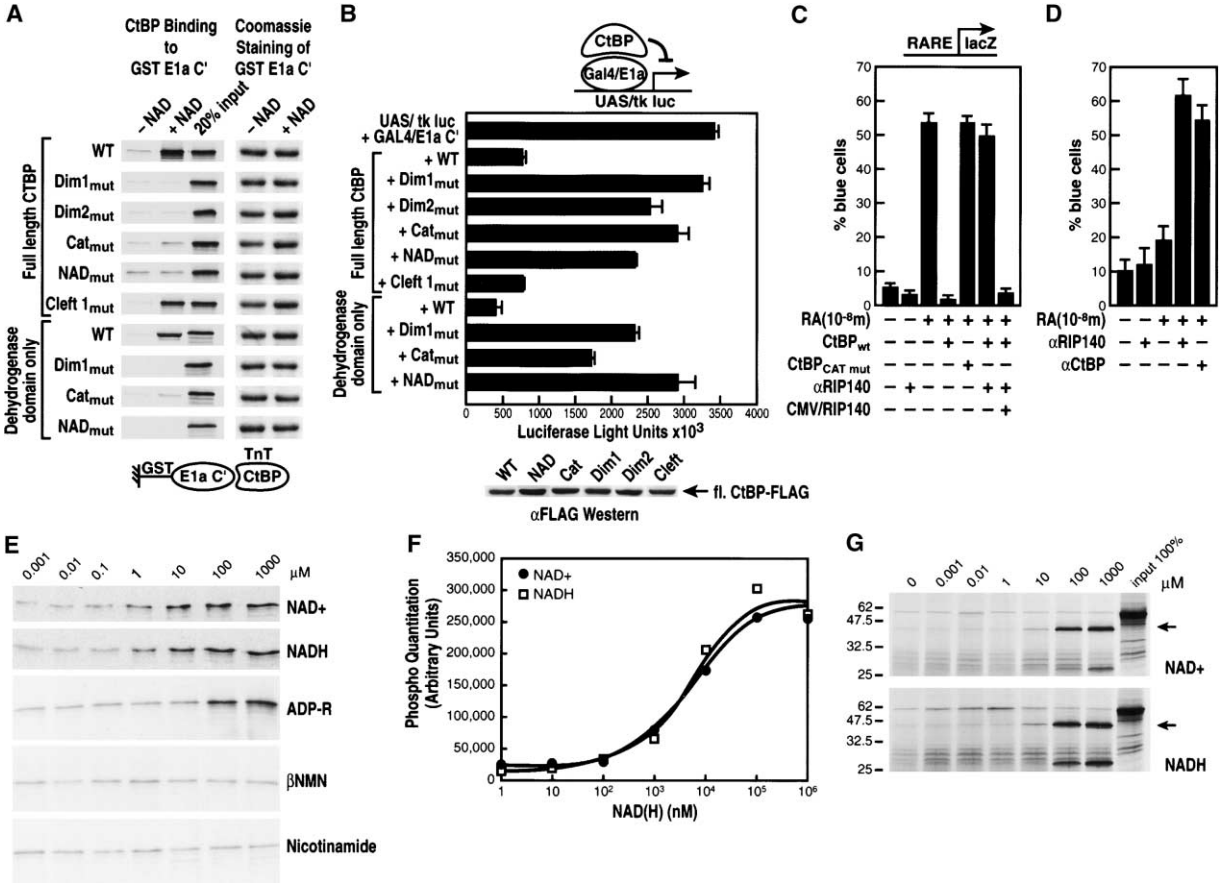

Figure 5. NAD^+ and NADH Enhance Binding of CtBP to E1A, and This Binding and Functional Repression Requires Residues in the Catalytic, NAD^+ Binding, and Dimerization Domains of CtBP

(A) GST E1A C′ was used to the test the binding of various mutants of CtBP in the presence or absence of 1 mM NAD^+/NADH. Addition of NAD^+/NADH consistently causes a marked enhancement of binding of wild-type (WT) CtBP holoprotein or the dehydrogenase domain only. Mutations that disrupt the dimerization, catalysis, or NAD^+ binding abolished the NAD^+. Panel on the right shows Coomassie staining of GST/E1A C′ as control for equal loading.

(B) Functional assay testing whether the mutants can repress Gal4/E1A C-based activation of UAS/tk luciferase. Both wild-type holoprotein and the dehydrogenase domain above were able to repress transcription; however the mutants impaired in PXDLS binding were unable to repress transcription. Expression levels of the various mutants were equivalent as seen by Western blot (Western blot panel below).

(C) CtBP inhibits ligand-dependent RAR activation via RIP140. Single-cell nuclear microinjection experiments were performed in Rat-1 cells. Addition of retinoic acid (RA 10^{-8} M) resulted in activation which was repressed by CMV/CtBP expression vector. This repression could be reversed by the addition of purified αRIP140 IgG and further restored by addition of CMV/RIP140 expression plasmid.

(D) Anti-CtBP IgG significantly reverses RIP-140-dependent suppression of RA-dependent gene activation, using the single-cell nuclear microinjection assay.

(E) GST E1A C′ binding to TnT CtBP at various concentrations of NAD^+, NADH, ADP-Ribose, βNMN, and Nicotinamide.

(F) Phosphoimager quantitation of the NAD^+ and NADH lanes in (E) demonstrating that NAD^+ and NADH are equally effective in stimulating the interaction.

(G) Protease digestion of TnT CtBP at various concentrations of NAD^+ and NADH. Upon cofactor binding and conformational change, a protease resistant 40 kDa band appears (arrow). Both NAD^+ and NADH are equivalently effective, and the band appears between 1 and 10 μM NAD(H). Results are shown as mean ± standard deviation and are representative of three independent experiments.

the active site residues. His315, Glu295, and Arg266 lie at the confluence of the NAD^+ and substrate binding domains and are in positions to interact with both a buried substrate and a PXDLS peptide segment at the rim of the active site cleft (Figures 3B and 4B). Interestingly, the active site cleft in the vicinity of His315, Glu295, and Arg266 is bordered by a loop from the 2-fold related CtBP subunit that could make additional contacts with the PXDLS motif (Figure 4B). The loss of these interactions, as in Dim_{mut}, could explain the importance of dimerization in E1A binding. To determine whether the CtBP mutants that were impaired in E1A binding were also defective in repression, we measured CtBP-dependent repression of Gal4/E1A on a UAS-tk-dependent reporter. Each set of mutations, except $Cleft_{mut}$, impaired the ability of expressed CtBP to repress Gal4/E1A, consistent with a failure to recruit E1A (Figure 5B). Moreover, when the mutant CtBP proteins were expressed at very high levels, they were able to repress Gal4/E1A, although not as efficiently as wild-type CtBP, arguing that these mutants still retain partial repressive function once bound to E1A.

CtBP Mediates RIP140-Dependent Repression In Vivo

Nuclear receptors bind p140 and p160 factors off and on DNA, and RIP140 appears to be the major p140 factor bound to LXXLL motifs (Cavailles et al., 1995; Heery et al., 1997; Torchia et al., 1997). However, RIP140, at best, is a weak activator (Cavailles et al., 1995). The observation that CtBP could bind to a variant PXDLS motif in RIP140 (Vo et al., 2001), and this interaction might be regulated by acetylation of an adjacent lysine residue (Zhang et al., 2000), prompted us to test the requirement for the catalytic residues of CtBP during repression by nuclear receptor. We found that increasing the levels of CtBP causes a complete block of ligand-dependent activation by retinoic acid receptor (Figure 5C). However, mutations of the catalytic residues (Cat_{mut}) abolished the ability of CtBP to induce repression, consistent with a role for this domain in recruitment of CtBP to the RAR activation complex. To determine whether this was dependent upon RIP140, the ability of a specific αRIP140 IgG to block CtBP-dependent repression was evaluated using single-cell microinjection assay. We found that injecting αRIP140 antibody fully restored the ligand-dependent activation and that the αRIP140 antibody had no effect on unliganded retinoic acid receptor transcription unit (Figure 5D). Thus, CtBP domains exhibited similar behavior for both E1A and RIP140-dependent repression events. Our results provide evidence that CtBP is a functional dehydrogenase and that it utilizes its dehydrogenase domain to bind to its recognition motif.

Biophysical and Biochemical Characterization of the Mutant Proteins

The mutations above were designed on the basis of the crystal structure to lie outside of the hydrophobic core, so as to preserve structure. The dimerization mutations were similarly designed to disrupt the dimer interface but not the monomeric structure. We confirmed the folding of Cat_{mut} and $Dim2_{mut}$ by circular dichroism (CD) spectroscopy, which monitors secondary structure. The far UV CD spectra of the dehydrogenase domains of wild-type CtBP, Cat_{mut}, and $Dim2_{mut}$ are similar, with the minima at 208 and 222 nm, characteristic of their α-helical content (Figure 6A). The depth of the 222 nm minimum is in approximate agreement with the helicity calculated from the crystal structure ($\sim$41% helicity). We tested dimerization capability by subjecting the dehydrogenase domains of Cat_{mut} and $Dim2_{mut}$ to analytical ultracentrifugation (AU). Equilibrium sedimentation data for Cat_{mut} provided a molecular mass ($\sim$74 kDa) that is in good agreement with the calculated size of a CtBP dehydrogenase domain dimer with an N-terminal his-tag ($\sim$76 kDa). $Dim2_{mut}$, however, could not be reliably analyzed by equilibrium sedimentation because the protein had a small tendency to precipitate over the long time period (13 hr) of data collection. Instead, we compared $Dim2_{mut}$ and Cat_{mut} by sedimentation velocity measurements with scans taken every 1 min over a period of 3 hr. The sedimentation velocity data for $Dim2_{mut}$, analyzed by the time derivative method (Philo, 2000), reveals a predominant peak with a sedimentation coefficient of 2.6S. This matches almost exactly the expected sedimentation coefficient for a CtBP monomer as calculated with the hydrodynamic modeling program HYDROPRO (Garcia de la Torre et al., 2000), using the coordinates for a CtBP monomer. In contrast, the predominant peak with Cat_{mut} has a sedimentation coefficient value of 4.1S, corresponding to a dimer. Together, these biophysical measurements show (i) that Cat_{mut} and $Dim2_{mut}$ are properly folded and (ii) that $Dim2_{mut}$ is compromised in its ability to dimerize.

Unlike Cat_{mut} and $Dim2_{mut}$, NAD_{mut} and $Dim1_{mut}$ expressed in inclusion bodies in *E. coli* that limited their biophysical analysis. As another measure of structure, we carried out partial proteolytic digestion of ^{35}S-labeled TnT mutant proteins in the apo form (Figure 6B). All the mutants, including NAD_{mut} and $Dim1_{mut}$, showed similar pattern of papain digestion as wild-type CtBP. We next showed that the Cat_{mut} was indeed defective in catalysis using the same pyruvate to lactic acid, coupled with NADH to NAD$^+$ assay (Figure 6C). We also carried out GST pull-down experiments with S^{35}-labeled TnT $Dim1_{mut}$ (and $Dim2_{mut}$) that is consistent with a lack of ability to dimerize (Figure 6D). We used the proteolysis assay to show that the NAD_{mut} does not bind NAD$^+$ (Figure 6E). As mentioned earlier, upon NAD$^+$ binding, there is a protease-resistant 40 kDa fragment of CtBP that is produced (Figure 6E, compare left panel, lanes 1 and 2); however, there is no such band in NAD_{mut} in the presence of NAD$^+$ (Figure 6E, compare right panel, lanes 1 and 2). In all, these biophysical and biochemical control experiments establish the structural integrity of the mutant proteins in assessing E1A binding in vitro and in vivo.

Discussion

The switch between transcriptional repression and transcriptional activation has been the subject of intensive investigation over the past 7 years, and one of the most intriguing aspects involves the identification of a number of enzymatic activities that underlie these events (Berger, 2001; Cheung et al., 2000; Kadonaga, 1998). The discovery of CtBP as a biologically critical corepressor, as genetically dissected in *Drosophila* (Nibu et al., 1998b), and the observation that it exhibits sequence homology to known D2-HDHs (Schaeper et al., 1995), has prompted the speculation that CtBP might contribute another important enzymatic activity to corepressor complexes. Here, we provide biochemical and structural evidence that CtBP is indeed a functional dehydrogenase, with a characteristic dumbbell shape and an active site cleft for NAD$^+$ and substrate binding. The dehydrogenase domain alone is sufficient to mediate repression and can bind the PXDLS recognition sequence motif of E1A in an NAD$^+$-dependent "closed" conformation. While a true substrate for CtBP remains to be identified, steric features of the substrate binding pocket suggest a D2-hydroxyacid with a small "R" group and the lack of a phosphate group.

CtBP has also been identified as brefeldin A ribosylation substrate (BARS50), whose LPA acyltransferase function is essential for Golgi maintenance (Spanfò et al., 1999; Weigert et al., 1999). The CtBP structure is inconsistent with a proposed acyltransferase reaction for CtBP/BARS in Golgi maintenance, in which acyl-CoA

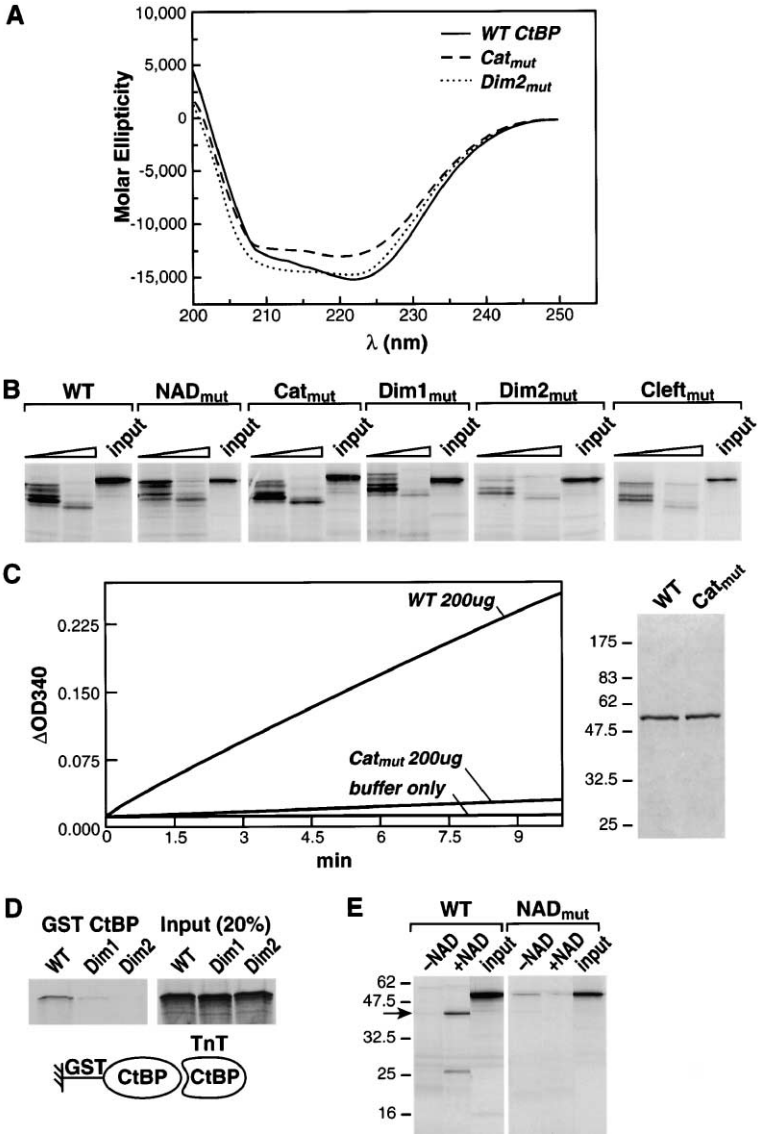

Figure 6. Biophysical and Biochemical Characterization of CtBP Mutants

(A) Far-UV CD spectra of wild-type CtBP (solid), Cat_{mut} (dashed), and $Dim2_{mut}$ (dotted). The mutant proteins have roughly equal secondary structure to wild-type CtBP.

(B) Partial protease digestion of the apo form of mutant CtBPs. TnT mutant proteins digested with papain have the same pattern as wild-type CtBP.

(C) CtBP Cat_{mut} is catalytically inactive. Bacterial wild-type and Cat_{mut} were prepared and used to convert pyruvate to lactic acid. The reaction was monitored by change in absorbance at 340 nM.

(D) $Dim1_{mut}$ and $Dim2_{mut}$ do not interact with wild-type CtBP. GST CtBP wild-type can bind with wild-type TnT CtBP but not the Dim mutants (compare lane 1 with 2 and 3).

(E) NAD_{mut} cannot bind NAD^+. Wild-type (WT) CtBP upon NAD^+ binding produces a protease-resistant 40 kDa fragment (left panel, compare lane 1 and 2, arrow indicates the 40 kDa fragment). NAD_{mut} protease digestion pattern is the same in the presence and absence of NAD^+, indicating that it cannot bind the cofactor.

is used to acylate lysophosphatidic acid to phosphatidic acid. It is not easy to see from our structure how both lysophosphatidic acid and acyl-CoA can be accommodated within the CtBP dehydrogenase active site. Moreover, the structure shows little relationship to that of glycerol-3-phosphate (1)-acyltransferase (Turnbull et al., 2001), which catalyzes an acyl-transfer reaction similar to that proposed for CtBP/BARS in the Golgi. However CtBP could carry out an NAD^+-dependent oxidation/reduction reaction in the Golgi that is more consistent with our structure. This could be true for both BARS50 as well as RIBEYE, which is a splice variation of CtBP2 consisting of an N terminus extension, found in synapses but whose function is unknown.

We show here that the dehydrogenase domain alone is sufficient to bind the PXDLS motif. This domain is highly conserved within CtBP family members from *C. elegans* to vertebrates. However the C terminus extension (C′) is highly variable with no predicted secondary structure. It is possible that C′ is a regulatory region, likely to mediate CtBP function after recruitment to a PXDLS motif. In *Drosophila*, there are three splice variants of CtBP differing only in the C′, and the shortest of these splice variants is essentially only composed of the dehydrogenase domain (Poortinga et al., 1998). We initially speculated, based on the crystal structure, that the PXDLS motif might bind in a cavity near the entrance to the active site cleft. However, mutations in this cavity do not disrupt E1A interactions in vitro or the repression function in vivo. Unexpectedly, mutation of the active site residues do affect E1A binding, suggesting that the PXDLS motif interacts with these residues at the periphery of the active site cleft. The cleft is walled off by a loop extending from the 2-fold related subunit that may provide additional interactions with the PXDLS sequence. Indeed, CtBP may be a simple dehydrogenase that has evolved or gained an extra ability to bind a PXDLS recognition motif.

The p140 is highly recruited to ligand receptors on cognate DNA sites (Cavailles et al., 1995). An interaction between CtBP and RIP140 has also been reported (Vo et al., 2001), which is intriguing because RIP140 is re-

cruited to nuclear receptors in response to ligand based on RIP140 LXXLL motifs; it competes with other coactivators (Heery et al., 1997). While at ambient levels of CtBP, liganded retinoic acid receptor induces recruitment of coactivators, including CBP, p160 factors (Glass and Rosenfeld, 2000); we show here that increased expression of CtBP completely blocks RAR activation, an effect entirely dependent on RIP140. Again, this effect requires specific CtBP catalytic residues, consistent with the expected role for these residues in stabilizing binding to interacting cofactors. This also implies that, in the presence of ligand, regulation of CtBP can be a key component to the nature of the transcriptional response.

The finding that E1A-CtBP requires NAD^+ has interesting implications. In particular, it raises the possibility that alterations in NAD^+ levels might modulate the binding of CtBP to specific repressor complexes, as well as regulating its own enzymatic activity. Alterations in NAD^+ level has been documented in response DNA damage, and the reported associations between CtBP and p130/Rb complex (Dahiya et al., 2001; Dick et al., 2000; Fusco et al., 1998; Meloni et al., 1999), BRCA1 (Li et al., 1999, 2000; Wong et al., 1998; Yu and Baer, 2000; Yu et al., 1998), and KU70 (Schaeper et al., 1998) may be critical regulatory components of cellular homeostasis. The ratio of NAD^+/NADH can vary in response to activation of metabolic dehydrogenases during day-night periods of food intake and starvation, and rhythmic cycles in the cellular redox state have been shown to regulate DNA binding of Clock and NPAS2 heterodimeric transcription factors (Rutter et al., 2001).

Using CtBP prepared and expressed in a mammalian system, we investigated whether E1A-CtBP interaction is regulated differently by NADH versus NAD^+ but found no evidence for it. Intriguingly, these results differ from those reported recently by Zhang et al. (2002) for a bacterially expressed CtBP, where NADH is two to three orders of magnitude more effective than NAD^+ in stimulating CtBP-E1A interaction (Zhang et al., 2002). This discrepancy may reflect different sources of CtBP; as we used in vitro transcribed and translated (TnT) CtBP, while Zhang et al. (2002) used bacterially expressed CtBP. The rabbit reticulocyte lysate used for the TnT reaction is known to posttranslationally modify proteins, including phosphorylation, acetylation, and isoprenylation. It is possible that one or more of these modifications dampen the differential effect observed with bacterial CtBP. In all, it is not easy to see from the structure how NADH could be up to three orders of magnitude more effective than NAD^+ in stimulating E1A-CtBP interaction, considering that the two cofactors differ chemically by only a hydrogen atom on the nicotinamide ring. This may be further clarified by comparing our structure to a complex of CtBP with NADH.

CtBP is not the only transcription corepressor to be now shown to bind NAD^+. The Sir2 family of transcriptional corepressors also binds NAD^+ as a cofactor for histone deacetylation reactions (Finnin et al., 2001; Min et al., 2001; Moazed, 2001; Shore, 2000), and furthermore, there is direct evidence that activity of NAD^+-dependent Sir2 repressors can regulate life span in *C. elegans* (Tissenbaum and Guarente, 2001). Whether levels of nuclear NAD^+ vary during development, viral infection, or transcriptional silencing remains to be determined, but it marks an intriguing new direction of future research.

Experimental Procedures

Protein Interaction Studies

GST fusion proteins (pGEX AHK-E1AC′ aa222-end; Amersham-Pharmacia) were purified and GST pull-down assays were performed according to previously described techniques (Horlein et al., 1995). GST pull-down assays were performed in PPI250 (20 mM HEPES, pH 7.9, 250 mM NaCl, 1 mM EDTA, 1 mM DTT, 0.05% NP40, 10% glycerol, and 1 mg/ml BSA). GST protein was blocked in PPI250 buffer 1 hr, bound to TnT proteins for 1 hr at 4°C, and followed by washes (5 × 10 min each) with PPI250. For experiments using NAD^+ (Sigma N6522), and NADH (Sigma N8129), ADP-Ribose (Sigma A0752), βNMN (Sigma N3501), and nicotinamide (Sigma N5535), all compounds were added to PPI250 buffer at the blocking step and then maintained throughout the following steps. For peptide competition, 10 μg of PXDLS peptide (EQTVPLDLSCKRPR), from E1A, was added during the binding step.

Dehydrogenase Assay

Assays were conducted in 0.2 M TrisCl, pH 7.3, with 20 mM NaPyruvate and 0.132 mM NADH at 25°C with the appropriate amount of baculovirus CtBP (Adams et al., 1973). The absorbance was measured at 340 nM in a UVKON XL spectrophotometer. Baculovirus CtBP was prepared using the BactoBac system from GIBCO-BRL.

Protease Digestion Protocol

^{35}S-labeled TnT CtBP was digested with limited amount of Papain (2 μg/ml and 0.6 μg/ml), for partial digestion, and higher levels (20 μg/ml) for complete digestion, in reaction buffer (100 mM Tris, pH 7.0, 150 mM NaCl, 2 mM EDTA, 2 mM βMe) for 30 min at 37°C. Where needed, the reaction buffer was complimented with the appropriate amount of NAD(H). The digested material was electrophoresed on a 15% SDSPAGE gel, dried, and exposed to film.

Transfections and Single-Cell Microinjection

All transfections were performed using HEK293 cells in 12-well plates. 0.3 μg of UAStk-Luciferase, 0.3 μg of Gal/E1A, and 50 ng of CMV/CtBP were used per well. Cells were transfected with $CaPO_4$ and harvested 24 hr later. Transfections were normalized using β-actin lacZ plasmid. Microinjections into Rat-1 cells were performed as previously reported (Torchia et al., 1997).

Crystallization

The minimal CtBP dehydrogenase domain (aa 28–353) was subcloned into the T7 expression vector pET15b (Novagen), and then following expression in *E. coli* BL-21(DE3) pLysS cells, the protein was purified in the presence of NAD^+ over a Ni^{2+} column. The selenomethionine (Semet)-substituted CtBP was purified similarly from *E. coli* B834, a methionine auxotrophic strain. Hexagonal crystals of the CtBP/NAD^+ complex were obtained from solutions containing 140 mM sodium formate, 70 mM magnesium acetate, and 100 mM Hepes (pH 7.0). The crystals belong to space group $P6_422$ with unit cell dimension of a = b = 89.1 Å, c = 164 Å, α = β = 90°, γ =120°. A Vm calculation of 2.47 $Å^3$/Da indicates a monomer in the asymmetric unit with 48% solvent in the crystal.

Data Collection, Structure Determination, and Refinement

Data on native crystals were collected at Brookhaven National Laboratory (BNL, beamline X25), extending to 1.95 Å resolution (Table 1). MAD data were collected at the Advanced Photon Source (APS, beamline ID32) at 3 wavelengths, corresponding to the edge, peak, and a high-energy remote point of the selenium K-edge absorption profile (Table 1). CNS (Brunger et al., 1998) was used to generate the initial experimental phases to 2.8 Å resolution, using the selenium data. The phases were extended to the 1.95 Å resolution limit of the native data using solvent flattening, which yielded a readily interpretable electron density map. The initial model built had an R factor of 47.1% (R_{free} of 47.0%). After a round of simulated annealing, energy minimization, and B factor refinement using CNS, the R factor

dropped to 34.8% (R_{free} 37.4%). NAD^+ was built into well-defined density in a Fo-Fc map. Iterative rounds of model building and refinement lowered the R_{free} to 30.0%, at which point waters were added. The final model contains a methionine from pET15b, CtBP residues from Pro28 to Asp352, NAD^+, and 414 waters.

CD Spectroscopy

Far UV CD spectra were collected on the bacterially expressed dehydrogenase domains of wild-type CtBP, Cat_{mut}, and $Dim2_{mut}$ on a Jasco-810 spectropolarimeter. The concentrations of wild-type CtBP, Cat_{mut}, and $Dim2_{mut}$ were 5.7, 9.3, and 4.9 μM, respectively. Relative ellipticity was converted to molar ellipticity.

Analytical Ultracentrifugation

Sedimentation equilibrium data on Cat_{mut} were measured on a Beckman XL-I analytical ultracentrifuge (An-60 Ti rotor). The experimental data were fitted using the WinNONLR package (http://Spin6.mcb.uconn.edu) and the molecular mass calculated by SEDNTRP (http://www.bbri.org/rasmb/rasmb.html). Sedimentation velocity data on $Dim2_{mut}$ and Cat_{mut} were recorded (AT-60 rotor, 42,000 rpm) by taking scans every 1 min for 3 hr, in both the absorbance and interference modes. The data were interpreted using the time derivative of the concentration profile g(s*) with the program $dcdt^+$ (Philo, 2000). The hydrodynamic modeling was done with programs HYDROPRO (Garcia de la Torre et al., 2000) using the CtBP crystal coordinates.

Acknowledgments

We are grateful to K. D'Amico for synchrotron time at the APS. We thank L. Shapiro and T. Boggon for help with data collection. We thank L. van Grunsven, C. Svensson, and A. Sundqvist for hCtBP1 and CtBP2 expression plasmids, respectively. We thank C. Nelson for tissue culture assistance, P. Meyer for illustrations, and M. Fischer for help with the manuscript. We also thank O. Hermanson and other members of the Rosenfeld Lab for support and encouragement. This research was supported by NIH grants to M.G.R and A.K.A. M.G.R is an investigator of the HHMI.

Received: December 5, 2001
Revised: August 13, 2002

References

Adams, M.J., Buehner, M., Chandrasekhar, K., Ford, G.C., Hackert, M.L., Liljas, A., Rossmann, M.G., Smiley, I.E., Allison, W.S., Everse, J., et al. (1973). Structure-function relationships in lactate dehydrogenase. Proc. Natl. Acad. Sci. USA *70*, 1968–1972.

Berger, S.L. (2001). An embarrassment of niches: the many covalent modifications of histones in transcriptional regulation. Oncogene *20*, 3007–3013.

Boyd, J.M., Subramanian, T., Schaeper, U., La Regina, M., Bayley, S., and Chinnadurai, G. (1993). A region in the C-terminus of adenovirus 2/5 E1a protein is required for association with a cellular phosphoprotein and important for the negative modulation of T24-ras mediated transformation, tumorigenesis and metastasis. EMBO J. *12*, 469–478.

Brunger, A.T., Adams, P.D., Clore, G.M., Delano, W.L., Gros, P., Grosse-Kunstleve, R., Jiang, W., Kuszewski, J., Nilges, M., Pannu, N.S., et al. (1998). Crystallography & NMR system: a software suite for macromolecular structure determination. Acta Crystallogr. D *54*, 905–921.

Cavailles, V., Dauvois, S., L'Horset, F., Lopez, G., Hoare, S., Kushner, P.J., and Parker, M.G. (1995). Nuclear factor RIP140 modulates transcriptional activation by the estrogen receptor. EMBO J. *14*, 3741–3751.

Cheung, P., Allis, C.D., and Sassone-Corsi, P. (2000). Signaling to chromatin through histone modifications. Cell *103*, 263–271.

Chinnadurai, G. (2002). CtBP, an unconventional transcriptional corepressor in development and oncogenesis. Mol. Cell *9*, 213–224.

Dahiya, A., Wong, S., Gonzalo, S., Gavin, M., and Dean, D.C. (2001). Linking the Rb and polycomb pathways. Mol. Cell *8*, 557–569.

Dengler, U., Niefind, K., Kiess, M., and Schomburg, D. (1997). Crystal structure of a ternary complex of D-2-hydroxyisocaproate dehydrogenase from Lactobacillus casei, NAD+ and 2-oxoisocaproate at 1.9 A resolution. J. Mol. Biol. *267*, 640–660.

Dick, F.A., Sailhamer, E., and Dyson, N.J. (2000). Mutagenesis of the pRB pocket reveals that cell cycle arrest functions are separable from binding to viral oncoproteins. Mol. Cell. Biol. *20*, 3715–3727.

Eklund, H., and Branden, C.I. (1987). Crystal structure, coenzyme conformations and protein interactions. In Pyridine Nucleotide Coenzymes, D.N.Y. Dolphin, ed. (New York: Wiley), pp. 51–98.

Finnin, M.S., Donigian, J.R., and Pavletich, N.P. (2001). Structure of the histone deacetylase SIRT2. Nat. Struct. Biol. *8*, 621–625.

Fusco, C., Reymond, A., and Zervos, A.S. (1998). Molecular cloning and characterization of a novel retinoblastoma-binding protein. Genomics *51*, 351–358.

Garcia de la Torre, J., Huertos, M.L., and Carrasco, B. (2000). Calculation of hydrodynamic properties of globular proteins from their atomic-level structure. Biophys. J. *78*, 719–730.

Glass, C.K., and Rosenfeld, M.G. (2000). The coregulator exchange in transcriptional functions of nuclear receptors. Genes Dev. *14*, 121–141.

Goldberg, J.D., Yoshida, T., and Brick, P. (1994). Crystal structure of a NAD-dependent D-glycerate dehydrogenase at 2.4 Å resolution. J. Mol. Biol. *236*, 1123–1140.

Grau, U.M., Trommer, W.E., and Rossmann, M.G. (1981). Structure of the active ternary complex of pig heart lactate dehydrogenase with S-lac-NAD at 2.7 Å resolution. J. Mol. Biol. *151*, 289–307.

Gray, S., and Levine, M. (1996). Transcriptional repression in development. Curr. Opin. Cell Biol. *8*, 358–364.

Heery, D.M., Kalkhoven, E., Hoare, S., and Parker, M.G. (1997). A signature motif in transcriptional co-activators mediates binding to nuclear receptors. Nature *387*, 733–736.

Hendrickson, W.A. (1991). Determination of macromolecular structures from anomalous diffraction of synchrotron radiation. Science *254*, 51–58.

Horlein, A.J., Naar, A.M., Heinzel, T., Torchia, J., Gloss, B., Kurokawa, R., Ryan, A., Kamei, Y., Soderstrom, M., Glass, C.K., et al. (1995). Ligand-independent repression by the thyroid hormone receptor mediated by a nuclear receptor co-repressor. Nature *377*, 397–404.

Jenuwein, T., and Allis, C.D. (2001). Translating the histone code. Science *293*, 1074–1080.

Kadonaga, J.T. (1998). Eukaryotic transcription: an interlaced network of transcription factors and chromatin-modifying machines. Cell *92*, 307–313.

Lamzin, V.S., Dauter, Z., Popov, V.O., Harutyunyan, E.H., and Wilson, K.S. (1994). High resolution structures of holo and apo formate dehydrogenase. J. Mol. Biol. *236*, 759–785.

Li, S., Chen, P.L., Subramanian, T., Chinnadurai, G., Tomlinson, G., Osborne, C.K., Sharp, Z.D., and Lee, W.H. (1999). Binding of CtIP to the BRCT repeats of BRCA1 involved in the transcription regulation of p21 is disrupted upon DNA damage. J. Biol. Chem. *274*, 11334–11338.

Li, S., Ting, N.S., Zheng, L., Chen, P.L., Ziv, Y., Shiloh, Y., Lee, E.Y., and Lee, W.H. (2000). Functional link of BRCA1 and ataxia telangiectasia gene product in DNA damage response. Nature *406*, 210–215.

Meloni, A.R., Smith, E.J., and Nevins, J.R. (1999). A mechanism for Rb/p130-mediated transcription repression involving recruitment of the CtBP corepressor. Proc. Natl. Acad. Sci. USA *96*, 9574–9579.

Min, J., Landry, J., Sternglanz, R., and Xu, R.M. (2001). Crystal structure of a SIR2 homolog-NAD complex. Cell *105*, 269–279.

Moazed, D. (2001). Enzymatic activities of Sir2 and chromatin silencing. Curr. Opin. Cell Biol. *13*, 232–238.

Nibu, Y., Zhang, H., Bajor, E., Barolo, S., Small, S., and Levine, M. (1998a). dCtBP mediates transcriptional repression by Knirps, Kruppel and Snail in the Drosophila embryo. EMBO J. *17*, 7009–7020.

Nibu, Y., Zhang, H., and Levine, M. (1998b). Interaction of short-

range repressors with Drosophila CtBP in the embryo. Science *280*, 101–104.

Pazin, M.J., and Kadonaga, J.T. (1997). What's up and down with histone deacetylation and transcription? Cell *89*, 325–328.

Philo, J.S. (2000). A method for directly fitting the time derivative of sedimentation velocity data and an alternative algorithm for calculating sedimentation coefficient distribution functions. Anal. Biochem. *279*, 151–163.

Poortinga, G., Watanabe, M., and Parkhurst, S.M. (1998). Drosophila CtBP: a Hairy-interacting protein required for embryonic segmentation and hairy-mediated transcriptional repression. EMBO J. *17*, 2067–2078.

Rao, S.T., and Rossmann, M.G. (1973). Comparison of super-secondary structures in proteins. J. Mol. Biol. *76*, 241–256.

Rutter, J., Reick, M., Wu, L.C., and McKnight, S.L. (2001). Regulation of clock and NPAS2 DNA binding by the redox state of NAD cofactors. Science *293*, 510–514.

Schaeper, U., Boyd, J.M., Verma, S., Uhlmann, E., Subramanian, T., and Chinnadurai, G. (1995). Molecular cloning and characterization of a cellular phosphoprotein that interacts with a conserved C-terminal domain of adenovirus E1A involved in negative modulation of oncogenic transformation. Proc. Natl. Acad. Sci. USA *92*, 10467–10471.

Schaeper, U., Subramanian, T., Lim, L., Boyd, J.M., and Chinnadurai, G. (1998). Interaction between a cellular protein that binds to the C-terminal region of adenovirus E1A (CtBP) and a novel cellular protein is disrupted by E1A through a conserved PLDLS motif. J. Biol. Chem. *273*, 8549–8552.

Schmitz, F., Königstorfer, A., and Südhof, T.C. (2000). RIBEYE, a component of synaptic ribbons: a protein's journey through evolution provides insight into synaptic ribbon function. Neuron *28*, 857–872.

Schuller, D.J., Grant, G.A., and Banaszak, L.J. (1995). The allosteric ligand site in the Vmax-type cooperative enzyme phosphoglycerate dehydrogenase. Nat. Struct. Biol. *2*, 69–76.

Shore, D. (2000). The Sir2 protein family: a novel deacetylase for gene silencing and more. Proc. Natl. Acad. Sci. USA *97*, 14030–14032.

Spanfò, S., Silletta, M.G., Colanzi, A., Alberti, S., Fiucci, G., Valente, C., Fusella, A., Salmona, M., Mironov, A., Luini, A., et al. (1999). Molecular cloning and functional characterization of brefeldin A-ADP-ribosylated substrate. A novel protein involved in the maintenance of the Golgi structure. J. Biol. Chem. *274*, 17705–17710.

Stoll, V.S., Kimber, M.S., and Pai, E.F. (1996). Insights into substrate binding by D-2-ketoacid dehydrogenases from the structure of Lactobacillus pentosus D-lactate dehydrogenase. Structure *4*, 437–447.

Tissenbaum, H.A., and Guarente, L. (2001). Increased dosage of a sir-2 gene extends lifespan in Caenorhabditis elegans. Nature *410*, 227–230.

Torchia, J., Rose, D.W., Inostroza, J., Kamei, Y., Westin, S., Glass, C.K., and Rosenfeld, M.G. (1997). The transcriptional co-activator p/CIP binds CBP and mediates nuclear-receptor function. Nature *387*, 677–684.

Turnbull, A.P., Rafferty, J.B., Sedelnikova, S.E., Slabas, A.R., Simon, J.W., Fawcett, T., Nishida, I., Murata, N., and Rice, D.W. (2001). Analysis of the structure, substrate specificity, and mechanism of squash glycerol-3-phosphate (1)-acyltransferase. Structure *9*, 347–353.

Turner, J., and Crossley, M. (2001). The CtBP family: enigmatic and enzymatic transcriptional co-repressors. Bioessays *23*, 683–690.

Tyler, J.K., and Kadonaga, J.T. (1999). The "dark side" of chromatin remodeling: repressive effects on transcription. Cell *99*, 443–446.

Vo, N., Fjeld, C., and Goodman, R.H. (2001). Acetylation of nuclear hormone receptor-interacting protein RIP140 regulates binding of the transcriptional corepressor CtBP. Mol. Cell. Biol. *21*, 6181–6188.

Weigert, R., Silletta, M.G., Spanò, S., Turacchio, G., Cericola, C., Colanzi, A., Senatore, S., Mancini, R., Polishchuk, E.V., Salmona, M., et al. (1999). CtBP/BARS induces fission of Golgi membranes by acylating lysophosphatidic acid. Nature *402*, 429–433.

Wong, A.K., Ormonde, P.A., Pero, R., Chen, Y., Lian, L., Salada, G., Berry, S., Lawrence, Q., Dayananth, P., Ha, P., et al. (1998). Characterization of a carboxy-terminal BRCA1 interacting protein. Oncogene *17*, 2279–2285.

Yu, X., and Baer, R. (2000). Nuclear localization and cell cycle-specific expression of CtIP, a protein that associates with the BRCA1 tumor suppressor. J. Biol. Chem. *275*, 18541–18549.

Yu, X., Wu, L.C., Bowcock, A.M., Aronheim, A., and Baer, R. (1998). The C-terminal (BRCT) domains of BRCA1 interact in vivo with CtIP, a protein implicated in the CtBP pathway of transcriptional repression. J. Biol. Chem. *273*, 25388–25392.

Zhang, Q., Yao, H., Vo, N., and Goodman, R.H. (2000). Acetylation of adenovirus E1A regulates binding of the transcriptional corepressor CtBP. Proc. Natl. Acad. Sci. USA *97*, 14323–14328.

Zhang, Q., Piston, D.W., and Goodman, R.H. (2002). Regulation of corepressor function by nuclear NADH. Science *295*, 1895–1897.